Abstract word count: 290 Manuscript word count: 4419
Display items: 4 Reference count: 48

Leveraging cancer mutation data to predict the pathogenicity of germline missense variants

Bushra Haque[1,2], David Cheerie[1,2], Amy Pan[2], Meredith Curtis[1,2], Thomas Nalpathamkalam[3], Jimmy Nguyen[1,2], Celine Salhab[1,2], Bhooma Thiruvahindrapura[3], Jade Zhang[4], Madeline Couse[5], Taila Hartley[6], Michelle M. Morrow[7], E Magda Price[6], Susan Walker[8], David Malkin[9], Frederick P. Roth[2,10-13], Gregory Costain[1-3,14]

[1]Program in Genetics and Genome Biology, SickKids Research Institute, Toronto, ON, Canada
[2]Department of Molecular Genetics, University of Toronto, Toronto, ON, Canada
[3]The Centre for Applied Genomics, The Hospital for Sick Children, Toronto, ON, Canada
[4]Human Biology Program, University of Toronto, Toronto, Ontario, Canada
[5] Centre for Computational Medicine, Hospital for Sick Children, Toronto, ON, Canada
[6]Children's Hospital of Eastern Ontario Research Institute, University of Ottawa, Ottawa, Ontario, Canada
[7]GeneDx, Gaithersburg, Maryland, USA
[8]Genomics England, London, United Kingdom
[9]Division of Haematology/Oncology, The Hospital for Sick Children, Department of Pediatrics, University of Toronto, Toronto, Ontario, Canada
[10]Donnelly Centre for Cellular and Biomolecular Research (CCBR), University of Toronto, Toronto, Ontario, Canada
[11]Lunenfeld-Tanenbaum Research Institute (LTRI), Sinai Health System, Toronto, Ontario, Canada
[12]Center for Cancer Systems Biology (CCSB), Dana-Farber Cancer Institute, Boston, MA, USA
[13]Department of Computer Science, University of Toronto, Toronto, Ontario, Canada
[14]Division of Clinical and Metabolic Genetics, The Hospital for Sick Children, and Department of Paediatrics, University of Toronto, Toronto, ON, Canada

Address correspondence to: Gregory Costain, gregory.costain@sickkids.ca

Short title: Predicting germline variant pathogenicity using cancer mutations

Keywords: missense variants; variant interpretation; rare disease; cancer; databases

ABSTRACT
Innovative and easy-to-implement strategies are needed to improve the pathogenicity assessment of rare germline missense variants. Somatic cancer driver mutations identified through large-scale tumor sequencing studies often impact genes that are also associated with rare Mendelian disorders. The use of cancer mutation data to aid in the interpretation of germline missense variants, regardless of whether the gene is associated with a hereditary cancer predisposition syndrome or a non-cancer-related developmental disorder, has not been systematically assessed. We extracted putative cancer driver missense mutations from the Cancer Hotspots database and annotated them as germline variants, including presence/absence and classification in ClinVar. We trained two supervised learning models (logistic regression and random forest) to predict variant classifications of germline missense variants in ClinVar using Cancer Hotspot data (training dataset). The performance of each model was evaluated with an independent test dataset generated in part from searching public and private genome-wide sequencing datasets from ~1.5 million individuals. Of the 2,447 cancer mutations, 691 corresponding germline variants had been previously classified in ClinVar: 426 (61.6%) as likely pathogenic/pathogenic, 261 (37.8%) as uncertain significance, and 4 (0.6%) as likely benign/benign. The odds ratio for a likely pathogenic/pathogenic classification in ClinVar was 28.3 (95% confidence interval: 24.2-33.1, $p < 0.001$), compared with all other germline missense variants in the same 216 genes. Both supervised learning models showed high correlation with pathogenicity assessments in the training dataset. There was high area under precision-recall curve values of 0.847 and 0.829 for logistic regression and random forest models, respectively, when applied to the test dataset. With the use of cancer and germline datasets and supervised learning techniques, our study shows that cancer mutation data can be leveraged to improve the interpretation of germline missense variation potentially causing rare Mendelian disorders.

AUTHOR SUMMARY
Our study introduces an approach to improve the interpretation of rare genetic variation, specifically missense variants that can alter proteins and cause disease. We found that genetic mutations identified in cancer have also been observed as germline variants that cause rare inherited (Mendelian) disorders. By using publicly available datasets, we observed that cancer mutations often overlap with rare germline variants associated with inherited disorders. This intersection led us to employ machine learning techniques to assess how cancer mutation data can predict the pathogenicity of germline variants. We trained machine learning models and tested them on a separate dataset curated by searching public and private genome-wide sequencing datasets from over a million participants. Our models were able to successfully identify pathogenic genetic changes, demonstrating strong performance in predicting disease-causing variants. This study highlights that cancer mutation data can enhance the interpretation of rare missense variants, aiding in the diagnosis and understanding of rare diseases. Integrating this approach into current genetic classification frameworks would be beneficial and opens new avenues for leveraging existing cancer research to benefit broader genetic studies and enhance medical diagnoses for rare genetic conditions.

BACKGROUND

Genome-wide sequencing (GWS; including exome and genome sequencing) allows for comprehensive detection of coding sequence variants associated with a wide range of diseases, spanning from rare Mendelian disorders to common cancers.[1–3] Our ability to filter and prioritize variants associated with disease lags behind our ability to detect variation.[2] Rare missense variants are collectively common in every human genome,[3,4] and interpreting the clinical impact of these variants is especially challenging. The American College of Medical Genetics and Genomics (ACMG) and the Association for Molecular Pathology (AMP) developed a widely used system for assessing variants by scoring lines of evidence supporting variant pathogenicity or benign-ness.[4] Even after more than a decade of implementing and refining the ACMG/AMP classification system, variants of uncertain significance (VUS) account for the vast majority of missense variant entries in databases like ClinVar.[5,6] Despite commendable efforts to generate functional data through multiplexed assays of variant effects (MAVEs) and other variant-to-function maps, missense variant classification in clinical practice continues to often rely on *in silico* evidence and heuristics like rarity and inheritance.[7,8] New scalable and easy-to-implement strategies that produce evidence complementary to (and not derivative of) existing *in silico* methods are needed to improve the pathogenicity assessment of rare germline missense variants.

Using widely available but underused genomic databases to identify additional evidence for pathogenicity could aid in classifying rare missense variants.[8–10] Tumour sequencing initiatives like The Cancer Genome Atlas (TCGA) and International Cancer Genome Consortium (ICGC) have accelerated the identification of oncogenic (cancer driver) mutations.[3,11] Germline dysregulation of some proto-oncogenes and tumour suppressor genes (TSGs) causes Mendelian

disorders ("oncoprotein duality") (Figure 1A).[7,12–14] For instance, the somatic *HRAS*^{Q61K} missense mutation implicated in various types of cancers causes Costello syndrome (MIM #218040), a developmental disorder, when it occurs as a germline variant (Figure 1B).[15,16] These Mendelian disorders may or may not include cancer as a major phenotypic feature.[5,17–21] Walsh and colleagues previously explored the use of cancer mutational hotspots data for interpreting germline variants in genes causing cancer predisposition syndromes.[12] However, when and to what extent cancer driver mutations are pathogenic in germline contexts, for rare Mendelian disorders in general, remains unknown.

This study investigates the concept of oncoprotein variant duality, and specifically the degree to which germline variant classification could be informed by observations that the equivalent tumour mutation drives cancer. The underlying logic of our approach is that cancer driver mutations have functional consequences at the protein level, and those functional consequences are expected to be present regardless of whether the variant is observed in a somatic/mosaic/tissue-specific or constitutional/germline context. Through comparative analysis of Cancer Hotspots[22,23] (cancer mutations) and ClinVar[24] (restricting to germline variants), we developed and tested supervised learning models for predicting germline missense variant pathogenicity using cancer mutation data.

RESULTS

Association between cancer mutations from Cancer Hotspots and LP/P classification as germline variants

Putative driver mutations from Cancer Hotspots were extracted, annotated, and filtered to obtain a list of 2,447 missense mutations ("CH mutations") distributed across 216 genes (Figure 1C). Of these 216 genes, 41% are proto-oncogenes, 36% are tumour suppressor genes, and 15% can have either role, as determined by the Cancer Gene Census (Supplemental Figure 2).[25] Although Cancer Hotspots infers cancer driver status of a mutation from probabilistic arguments (statistical enrichment), we found that the functional impact was experimentally tested for 990 of these mutations with the majority (943/990, 95%) confirmed to result in gain or loss of protein function (Supplemental Methods; Supplemental Figure 3).

Overall, 691 missense mutations in 84 genes had been classified with respect to germline pathogenicity in ClinVar: 426 (61.6%) as LP/P, 261 (37.8%) as VUS, and 4 (0.6%) as LB/B (Figure 1C). As expected, all variants were rare (gnomAD allele frequency < 0.001) except for three out of four that were classified as LB/B. Reviewing the Mendelian disease associations in the Online Mendelian Inheritance in Man (OMIM) database[26] for these 84 genes revealed that 38% were hereditary cancer predisposition syndromes (e.g., *VHL* associated with von Hippel-Lindau syndrome) and 62% were not known to include cancer as a predominant feature (e.g., *FGFR3* associated with Achondroplasia). In both groups, most associated conditions had autosomal dominant inheritance (88% and 77%, respectively). A significant difference was observed in the proportion of LP/P, VUS, and LB/B variants between these two gene groups (256 LP/P, 231 VUS, 1 LB/B versus 169 LP/P, 29 VUS, 3 LB/B, respectively), with an LP/P classification more likely for variants in genes not associated with hereditary cancer predisposition syndromes ($p < 2.2e-16$).

The odds ratio for these 691 variants having a LP/P classification in ClinVar was 107.6 (95% confidence interval (CI): 40.1-288.4, $p < 0.0001$), when comparing only LP/P and LB/B classifications with all other germline missense variants with ClinVar entries in the 216 genes (n=5,474) (Supplemental Figure 1; Supplemental Table 1). Even if all VUS were considered as LB/B variants, the odds ratio was 28.3 (95% CI: 24.2-33.1, $p < 0.001$) compared with all other variants in ClinVar (n=50,655) (Supplemental Figure 1; Supplemental Table 1). In an even more extreme scenario of considering all VUS and CIP variants as LB/B, the odds ratio was 21.0 (95% CI: 18.2-24.2, $p < 0.001$) (n=53,593) (Supplemental Figure 1; Supplemental Table 1). The positive likelihood ratio of 11.4 exceeded "moderate evidence" thresholds described previously (i.e., 4.33 and 5.79).[27,28] The potential impact of an additional moderate evidence criterion for pathogenicity applied to the 261 CH mutations that overlap with germline VUS in ClinVar is shown in Supplemental Figure 4, revealing 66 (27%) of the VUS could be hypothetically upgraded to LP.

For the remaining CH mutations that did not overlap with germline variants in ClinVar (n = 1,756), we explored the degree to which *in silico* scores used for germline variant adjudication supported "pathogenicity". We grouped these CH mutations by REVEL scores using the ClinGen-proposed PP3/BP4 score thresholds (Figure 1C).[29] Over half (58.8%; 1,032) had REVEL scores indicating at least PP3-level evidence (i.e., evidence in favour of pathogenicity), while only 9.6% (168) had at least BP4-level evidence (Figure 1C; Supplemental Figure 5A). Findings were similar using AlphaMissense (Supplemental Figure 5B).[30] For these CH mutations that are absent from ClinVar, the *in silico* score profiles resemble the ClinVar LP/P germline

missense variants in the same genes more than the set of LB/B variants or VUS (Supplemental Figure 5).

Through collaborations with GEL, MSSNG, C4R, and GeneDx, we searched GWS datasets from approximately 1.5 million participants (probands and affected or unaffected family members) and identified additional instances of germline variants overlapping with CH mutations (Supplemental Table 2). Across the four datasets, we found 302 unique overlapping germline variants. Of these, 194 were already classified and present in ClinVar (140 LP/P, 1 LB/B, 53 VUS) and 108 were absent in ClinVar. Out of these 108 variants, 43 had been previously assessed and classified in accordance with ACMG/AMP variant interpretation guidelines by our collaborators. Among these variants, 30 were classified as LP/P, 12 as VUS, and 1 conflicting (LP and VUS by different groups). The classifications of the remaining 65 variants (79% found in probands) were uncertain due to limited phenotype information.

Cancer Hotspots database predominantly captures recurring (putative) cancer driver mutations

We retrieved 231,377 somatic missense mutations by filtering the Cancer Census Genes data from COSMIC (Supplemental Figure 6). With the results of the tumour sample count analysis using overlapping CH mutations and ClinVar germline variants (Supplemental Methods, Supplemental Figure 7), we stringently filtered for COSMIC mutations that were observed in >25 tumour samples and absent from Cancer Hotspots, resulting in 125 missense mutations across 63 genes (Supplemental Figure 6). Of these genes, 31 are new additions to the list of genes from Cancer Hotspots and 11 are associated with rare Mendelian diseases as reported in

OMIM.[26] However, only 12 of these mutations overlapped with germline variants in ClinVar. Among them, 2 (16.7%) were LP/P, 8 (66.7%) VUS/CIP and 2 (16.7%) were LB/B (Supplemental Figure 6). Only 2 of these 12 overlapping variants were found in the "new" 31 cancer genes discovered through COSMIC. While we identified 125 additional missense mutations in COSMIC, only a small fraction of these overlapped with germline variants in ClinVar, reinforcing the comprehensive coverage of Cancer Hotspots in cataloging putative cancer drivers.

Robust predicted probabilities of pathogenicity generated by supervised learning models

We used the training datasets to develop two types of supervised learning models with the goal to accurately predict the pathogenicity of germline variants in our test dataset. The training dataset fit the LRM with a McFadden's pseudo-R^2 value of 0.50 (i.e., higher than the 0.20-0.40 range that indicates a good model fit[31]) and generated predicted probabilities of pathogenicity for all variants in the training dataset. The predicted probabilities were significantly higher for all germline LP/P variants compared with LB/B/VUS variants ($U = 1655893$, $n_{LB/B/VUS} = 11{,}644$, $n_{LP/P} = 2{,}095$, $p < 0.0001$) and for germline variants that are present in the Cancer Hotspots database compared with those that are absent ($U = 32029$, $n_{Absent} = 13{,}316$, $n_{Present} = 423$, $p < 0.0001$) (Figure 3AB). We trained a second supervised learning model, an RFM, since it is gene-independent and can be broadly applied to variants beyond the 66 gene categories in the LRM. The RFM achieved an out-of-bag (OOB) error estimate of 10.8% for predicting outcomes. The RFM generated probability scores of pathogenicity and, similar to the LRM, these were significantly higher for all germline LP/P variants compared with LB/B/VUS variants, as well as for germline variants that overlap with CH mutations compared to those without overlap (U =

6109589, $n_{LB/B/VUS}$ = 11,644, $n_{LP/P}$ = 2,095, $p < 0.0001$) (Figure 3CD). To gain a comprehensive understanding of the overall impact of each independent variable on the data, exploratory analyses were conducted on the ClinVar dataset (before filtering) (Supplemental Methods; Supplemental Figures 6-8). The analyses show variability in the number of variants across genes (Supplemental Figure 7), distinct tumour sample count thresholds between LP/P and LB/B/VUS variants (Supplemental Figure 8) and indicated that the model fit was not primarily driven by the conservation scores (Supplemental Figure 9).

RFM outperformed LRM in predicting pathogenicity of germline missense variants overlapping with cancer mutations

Using the test dataset (n = 339), distinct from training dataset variants, we calculated the AUPRC values for the LRM and RFM as 0.847 and 0.829, respectively (Figure 4A). Precision-recall curves guided the selection of optimal classification thresholds, with an emphasis on minimizing false positives while maximizing AUPRCs. The LRM had an optimal threshold of 0.74 (F1 score = 0.690) (Supplemental Figure 10A). The RFM had an optimal threshold of 0.39 (F1 score = 0.783) (Supplemental Figure 10B), with the higher F1 score compared with the LRM indicating superior performance in predicting the pathogenicity of test dataset variants.

We compared the performance of the LRM and RFM pathogenicity scores against the scores of other *in silico* prediction tools by plotting precision-recall curves and comparing the calculated AUPRCs (Supplemental Figure 11A). The LRM and RFM outperformed the first-generation tools[32] SIFT and PolyPhen-2, which had AUPRCs of 0.821 and 0.827, respectively (Supplemental Figure 11B). Second- and third-generation[32] tools demonstrated a stronger

performance in classifying the test dataset variants, with AUPRCs ranging from 0.881 to 0.963 (Supplemental Figure 11CD). REVEL, VARITY, and AlphaMissense were the top-performing tools, respectively. Given the smaller size of the test dataset compared with the training dataset, cross-validation techniques were also used to confirm the LRM and RFM's reliability in estimating performance (Figure 4B). The RFM consistently outperformed the LRM, exhibiting a higher AUPRC than was observed with the test dataset alone (0.940 versus 0.738 AUC). We used the RFM and an optimal threshold value of 0.39 to predict pathogenicity of the 65 variants with unknown classification identified through our collaborations with MSSNG, GEL, C4R, and GeneDx. Of these 65 variants, the RFM predicted 92% to be LP/P and 8% as LB/B. The average probability score of pathogenicity for the predicted LP/P variants was 0.93 and 80% were in probands.

DISCUSSION

The increasing use of GWS in clinical practice has underscored the need for novel methods to interpret germline missense variation.[2,5,33] We explored the generalizability of an understudied line of evidence that considers overlap with (presumed driver) cancer mutations. Using 2,447 cancer missense mutations from the Cancer Hotspots database, we identified significant enrichment for LP/P germline variants causing rare Mendelian disorders, regardless of cancer being or not being a major phenotype of the disorder. We were successful in predicting the pathogenicity of germline missense variants using supervised learning models trained with CH mutation data. Our findings indicate that statistically significant recurrent cancer mutation data can be leveraged to improve the interpretation of germline missense variation potentially causing rare Mendelian disorders.

Walsh and colleagues first proposed modifying the existing PM1 pathogenic evidence criterion to apply to germline variants in cancer predisposition genes that overlap with cancer mutations from Cancer Hotspots,[12] provided the variant was not already in a germline hotspot.[4] The results of our study support and extend this concept. A majority (62%) of genes considered in our study are not known to be associated with hereditary/germline cancer predisposition in a Mendelian disease context. We emphasize that this line of evidence is not codified in existing interpretation frameworks, including ACMG, ClinGen, and the Association for Clinical Genomic Science (ACGS), and is distinct from other criteria specific to missense variants, such as germline mutational hotspots (PM1) and instances where a previous pathogenic variant has been previously observed (PS1/PM5). This evidence may be most relevant in scenarios involving the interpretation of (rare) missense VUS. The stand-alone probability scores of pathogenicity from our supervised learning models were not superior to other widely used *in silico* prediction tools in classifying germline missense variants. However, because our models are the first to be trained on somatic cancer mutation data, they demonstrate proof-of-concept, leverage orthogonal lines of evidence, and warrant consideration for use in aggregator tools. The supervised learning models in our study can be implemented using the training dataset, and subsequently applied to variants of interest prospectively to obtain probability scores of pathogenicity. While the LRM is restricted to the 66 genes constituting our training dataset, the RFM is not limited to these genes. Through our collaborations with MSSNG, C4R, GEL, and GeneDx, we identified an additional 65 individuals with suspected rare diseases and a germline variant that overlapped with a Cancer Hotspot mutation. Many of these cases remain “unsolved”, and the inclusion of this criterion may offer valuable insights for variant interpretation.

This study focused on missense variants because of the existence of a cancer driver missense mutation database and because of the large number of missense variants in ClinVar. We explored the potential application of using cancer missense mutations to inform germline variant interpretation to non-coding variants by leveraging mutation data from COSMIC and other putative cancer driver databases (Supplemental Methods). Results were inconclusive due to the limited availability of non-coding germline variants clinically classified in public databases (data not shown).

This study has several additional limitations. It primarily focused on a subset of cancer mutations from Cancer Hotspots, last updated in 2017. However, only a small fraction of the additional highly recurrent missense mutations present in COSMIC in 2024 overlapped with germline variants in ClinVar, suggesting that Cancer Hotspots remains a near comprehensive list of statistically recurring cancer (driver) mutations. We did not assess the oncogenicity of each cancer mutation in Cancer Hotspots.[34] It is possible that overlap with cancer mutations contributed to the clinical interpretation of some germline variants in ClinVar, despite such evidence not yet being codified in existing classification guidelines.[4,35,36] Of note, however, is that the term "Cancer Hotspots database" was only mentioned 3 times in the context of missense SNVs in the ClinVar database of 3,614,935 submitted records (search date: December 2023). In the training dataset, there was variability in the LRM's independent "gene" variable, leading to inconsistent performance across genes. We also did not explicitly consider the concordance of disease mechanism directionality (i.e., gain of function, loss of function) for the progression of cancer and for Mendelian disease. We recognize the potential relevance of this consideration,

particularly for germline missense variants with a gain of function mechanism, where *in silico* tools like REVEL demonstrate worse performance.[37] Further increasing the size of the test dataset was not possible; to compensate, cross-validation was used to evaluate model performance. Last, while we identified additional germline variants that overlap with CH mutations in private genomic datasets, we were not able to formally reclassify variants and return new information back to those individuals. However, the identified variants in the GEL Research Environment were shared with GEL for further review.

Our results demonstrate a modeling approach that uses overlapping cancer mutations to facilitate the interpretation of pathogenic germline missense variants. The presence of a variant in Cancer Hotspots suggests that additional published evidence from somatic cancer studies exists that may be relevant to understanding the impact of the same variant in a germline context. As we navigate the complexities of variant interpretation, leveraging the growing wealth of genomic data in both cancer and germline contexts will contribute to refining our understanding and improving diagnostic capabilities in the field of rare diseases.

METHODS

Extracting cancer mutation data from Cancer Hotspots

We obtained cancer mutation data for 3,122 single nucleotide variants (SNVs) from the Cancer Hotspots[22,23] database (www.cancerhotspots.org), representing a set of true cancer driver mutations. This database consists of mutational hotspots identified in large scale cancer genomics data, defined as single amino acid positions in protein-coding genes that are mutated more frequently than would be expected in the absence of selection.[12,23] This method assigns a

statistical significance to the recurrence of mutation at a given amino acid and is corrected for background mutational rate of the position, gene, and sample both within and across cancer types in the affected cohort.[22,23] Somatic mutational hotspots are therefore not common germline benign variants in a population.[12,22,23] A Python script was developed to extract genomic coordinates in GRCh37, reference and alternate alleles, and tumour sample counts for each mutation. Only missense mutations (n=2,576) were used for our analyses. We annotated the cancer missense mutations using ANNOVAR and a custom pipeline[2] developed by The Centre for Applied Genomics (Toronto, Canada). ClinVar annotations (date accessed: Jan 2022) were used to identify cancer mutations that have been observed as germline variants and clinically classified. We conservatively excluded any mutations with corresponding germline variants with "conflicting interpretations of pathogenicity" (CIP) or considered a "risk factor" for disease (n = 129). The remaining 2,447 recurrent missense mutations (n=216 total genes) from Cancer Hotspots are hereafter referred to as the "CH mutations".

Comparing cancer mutations with germline variants

Separately, we extracted from ClinVar (date accessed: Jan 2022) all missense variants in the 216 genes from the list of CH mutations (n = 51,346 SNVs) (Supplemental Figure 1). We selected missense variants with a "germline" allele origin, i.e., excluding those labeled as "somatic" or "unknown". These variants were then grouped into three categories based on their ACMG classification in ClinVar: "likely pathogenic" or "pathogenic" (LP/P) (n = 3,149), "likely benign" or "benign" (LB/B) (n = 2,755), and "variant of uncertain significance" (VUS) (n = 45,442). We annotated these variants using ANNOVAR to include REVEL[38], phyloP[39] (20way mammalian and 7way vertebrate), and phastCons[40] (20way mammalian and 7way vertebrate) scores. For

each variant, we noted the presence or absence of an overlap with a CH mutation. These variants are hereafter to as the "ClinVar dataset" and were used to calculate the odds ratio of a germline variant that overlaps with a CH mutation having an LP/P classification.

Identifying overlap with cancer mutations in other genomic databases

We queried the CH mutations in four controlled-access GWS databases, in collaboration with MSSNG[41], Genomics England[42] (GEL), Care4Rare[43] (C4R), and GeneDx[9,44], to identify matching germline missense variants (at the nucleotide level).

The MSSNG database represents a cohort of autistic individuals / individuals with autism and their family members. All germline missense variants in this database were extracted and converted to GRCh37 using LiftOver. Germline variants in MSSNG, and CH mutations, were imported to R version 4.1.0 (R Foundation for Statistical Computing) to identify overlapping variants by genomic coordinate, reference allele, and alternate allele. The GEL, C4R, and GeneDx databases represent phenotypically heterogeneous cohorts of individuals with suspected rare genetic diseases and their family members. In the GEL Research Environment, a bash shell script was used to extract small variants (SNVs and indels <50 bp) from variant call format (VCF) files by genomic coordinates. The CH mutations were queried against germline variants in the VCF files of all participants in the Rare Disease program using this script. The participant IDs for each CH mutation that overlapped with a germline variant were used to retrieve phenotype data along with their classifications using the Labkey platform. In collaboration with C4R and GeneDx, the CH mutations were sent to the respective study teams and queried within their databases. Results of overlapping variants and participant IDs were returned. Variant

classification and phenotype data from C4R was explored by searching the Genomics4RareDisease (G4RD) database with participant IDs.[45]

Identifying cancer mutations from other cancer databases and comparing with germline variants

We downloaded approximately 1.1 million coding mutations from the COSMIC database[46] listed in the Cancer Gene Census[25] and filtered for confirmed somatic missense mutations (n = 231, 477). To align with the stringent criteria used in the Cancer Hotspots database, we further filtered based on the presence of mutations in COSMIC across a defined number of tumor samples. This step ensured the retention of only those mutations observed across a substantial number of tumors, indicative of potential driver mutations as defined in Cancer Hotspots. For this filtering process, we used tumor sample counts of CH mutations that overlap with germline variants in ClinVar (Supplemental Methods). Plotting these values by ClinVar classification groups (LP/P and LB/B/VUS), we generated receiver operating characteristic (ROC) curves to determine the optimal tumor sample count cut-off for distinguishing between LP/P and LB/B/VUS variants. The identified optimal count was then used to filter the COSMIC mutations. We then conducted further filtered to identify "new" mutations in COSMIC, i.e., those absent in Cancer Hotspots, and compared these mutations with germline variants in ClinVar, to identify additional overlapping variants.

Training dataset used for supervised learning models

We developed supervised learning models to predict pathogenicity of unclassified germline variants, based on a set of variants with known classifications in ClinVar. To construct the

training variant set, we used the ClinVar dataset including n = 51,346 SNVs in the 216 genes from the list of CH mutations. Different nucleotide variants resulting in the same amino acid change were grouped together. VUS with REVEL scores >0.29 were excluded from the training dataset. The remaining VUS were included and treated as LB/B variants (Figure 2; see below regarding weighting), to address class imbalance arising from fewer LB/B versus LP/P variants in the dataset. Variants were then restricted to a set of 66 genes, determined by the updated list of 428 CH mutations overlapping with germline variants (Figure 2). The resulting training dataset comprises 13,881 variants.

Developing supervised learning models

Two types of supervised learning models were fit to the training dataset in R: a logistic regression model (LRM) and a random forest model (RFM). Pathogenicity status (LB/B, LP/P) was used as the dependent variable and the following were used as independent variables: 1) overlap with a cancer missense mutation from Cancer Hotspots (2 categories: present = 1, absent = 0), 2) the protein-coding gene associated with a variant (with 66 categories representing each gene), 3) the number of tumour samples with a specific amino acid change at a residue position from Cancer Hotspots, 4) the number of tumour samples with a mutated residue from Cancer Hotspots, 5 & 6) the phyloP conservation scores[39] (20way mammalian and 7way vertebrate), and 7 & 8) the phastCons conservation scores[40] (20way mammalian and 7way vertebrate).

The 'stats' R package was used to fit the LRM. REVEL scores for the included VUS (all <= 0.29) were used as prior weights (*weight* = 1 - *REVEL score*) compared to true LB/B variants (*weight* = 1). The predicted probabilities and standard performance metrics including Akaike Information

Criterion (AIC) and McFadden's pseudo-R^2 were used to assess the fit of the model. The same training dataset was used for the RFM using the 'randomForest' package in R. However, the gene variable was excluded due to a categorical variable limit of 32 levels. 350 classification trees were generated, and four independent variables were randomly selected as candidates for each split in the classification trees.

Evaluating supervised learning models with test dataset

Both LRM and RFM performance was evaluated using a test dataset of 339 germline missense variants that were absent from the training dataset. These variants were obtained from new ClinVar submissions from Feb 2022 to Aug 2022 (n = 189), the Leiden Open Variation Database (LOVD)[47] (n = 35), G4RD database[54] (n = 1), GEL database[48] (n = 93), SickKids Cancer Sequencing (KiCS) dataset[49] (n = 2), and from manual review of literature pertaining to the genes of interest that was published from 2021-2022 (n = 19). The test dataset variants impact genes that are represented in the training dataset. We used the predicted classifications of each model across all possible classification thresholds to plot precision-recall curves and calculate the area under the curve (AUPRC). The highest performing model and optimal threshold were used to assess the pathogenicity of an additional set of variants with unknown classification identified in other genomic databases through collaborations. The variants in the test dataset were annotated using scores from other *in silico* prediction tools, including SIFT[50], PolyPhen-2[51], REVEL[38], CADD[52], VARITY[53], AlphaMissense[30], and PrimateAI[10]. We also plotted precision-recall curves using these scores to calculate the AUPRCs and compared them with the LRM and RFM.

Evaluating supervised learning models with cross-validation

Cross-validation was conducted using the 'caret' package in R, with the 'createFolds' function employed to generate the folds for model training and evaluation. The training dataset was divided into *k* folds, where the model was trained on *k-1* fold and tested on the remaining one. The training dataset was divided into 8 and 10 folds for the LRM and RFM, respectively. The F1 score and AUPRC, using a threshold of 0.5, was calculated for each fold, and averaged over the *k* folds to obtain an estimate of each model's generalization ability.

Statistical methods

Standard descriptive statistics, odds ratios, and Mann-Whitney U tests were performed using R and GraphPad Prism 9 with two-tailed statistical significance set at $p < 0.05$.

LIST OF ABBREVIATIONS

DECLARATIONS

ETHICS DECLARATION

This secondary use data study was approved by the Research Ethics Board at the Hospital for Sick Children. The de-identified data from GeneDx was assessed in accordance with an IRB-approved protocol (WIRB #20171030).

AVAILABILITY OF DATA AND MATERIALS

The cancer mutation data from Cancer Hotspots that support the findings of this study are available through a public database and at the following URL: https://www.cancerhotspots.org/. Germline variants and their classifications are available in the ClinVar public archive: https://www.ncbi.nlm.nih.gov/clinvar/. For the Cancer Hotspots cancer mutation data transformation, the Python script is openly available on a GitHub repository: https://github.com/haqueb2/Cancer-Hotspots-Reformat. The training dataset used for training supervised learning models, the LRM and RFM pathogenicity scores assigned to training and test dataset variants, and prediction scores generated by other *in silico* tools for the test dataset are all available in Supplemental Table 3. R scripts used to train supervised learning models can be made available upon request. Datasets from Genomics England, MSSNG, Care4Rare, and GeneDx are not openly available due to controlled access requirements. Access to these datasets can be made available upon request to the respective organizations.

COMPETING INTERESTS

SW is an employee of Genomics England Limited. MMM is an employee of GeneDx, LLC. The remaining authors have no potential conflicts of interest to declare.

FUNDING

SickKids Research Institute, Canadian Institutes of Health Research, and the University of Toronto McLaughlin Centre. The funders had no role in the design and conduct of the study.

ACKNOWLEDGEMENTS

This research was made possible through access to data in the National Genomic Research Library, which is managed by Genomics England Limited (a wholly owned company of the Department of Health and Social Care). The National Genomic Research Library holds data provided by patients and collected by the NHS as part of their care and data collected as part of their participation in research. The National Genomic Research Library is funded by the National Institute for Health Research and NHS England. The Wellcome Trust, Cancer Research UK and the Medical Research Council have also funded research infrastructure. The authors wish to acknowledge the resources of MSSNG (www.mss.ng), Autism Speaks and The Centre for Applied Genomics at The Hospital for Sick Children, Toronto, Canada. We also thank the participating families for their time and contributions to this database, as well as the generosity of the donors who supported this program. This study makes use of data obtained through Care4Rare Canada studies (CHEO REB #11/04E and OGI-147) and shared via controlled access to Genomics4RD, a rare disease data sharing platform. We are grateful to the biostatisticians through the Clinical Research Core Facilities at the Hospital for Sick Children for their consultation on training data design and statistical analyses. We thank additional students affiliated with the Department of Molecular Genetics at the University of Toronto who provided helpful input on study design and analysis plans.

AUTHOR CONTRIBUTIONS

Conceptualization: GC

Data curation: BH, TM, BT, TH, MMM, EMP

Formal analysis: BH, DC, AP, MC, JN, CS, JZ

Funding acquisition: BH, GC

Supervision: GC, DM, FPR

Visualization: BH

Writing-original draft: BH, GC

Writing-review & editing: DC, AP, MC, TN, JN, CS, BT, JZ, TH, MMM, EMP, SW, DM, FPR

REFERENCES

1. Amberger, J. S., Bocchini, C. A., Scott, A. F. & Hamosh, A. OMIM.org: leveraging knowledge across phenotype-gene relationships. *Nucleic Acids Res* **47**, D1038–D1043 (2019).
2. Costain, G. *et al.* Genome Sequencing as a Diagnostic Test in Children With Unexplained Medical Complexity. *JAMA Network Open* **3**, e2018109 (2020).
3. Cancer Genome Atlas Research Network *et al.* The Cancer Genome Atlas Pan-Cancer analysis project. *Nat Genet* **45**, 1113–1120 (2013).
4. Richards, S. *et al.* Standards and guidelines for the interpretation of sequence variants: a joint consensus recommendation of the American College of Medical Genetics and Genomics and the Association for Molecular Pathology. *Genet Med* **17**, 405–423 (2015).
5. Fayer, S. *et al.* Closing the gap: Systematic integration of multiplexed functional data resolves variants of uncertain significance in BRCA1, TP53, and PTEN. *The American Journal of Human Genetics* **108**, 2248–2258 (2021).
6. Spielmann, M. & Kircher, M. Computational and experimental methods for classifying variants of unknown clinical significance. *Cold Spring Harb Mol Case Stud* **8**, a006196 (2022).
7. Qi, H., Dong, C., Chung, W. K., Wang, K. & Shen, Y. Deep Genetic Connection Between Cancer and Developmental Disorders. *Hum Mutat* **37**, 1042–1050 (2016).
8. Lal, D. *et al.* Gene family information facilitates variant interpretation and identification of disease-associated genes in neurodevelopmental disorders. *Genome Medicine* **12**, 28 (2020).
9. Haque, B. *et al.* A comparative medical genomics approach may facilitate the interpretation of rare missense variation. 2023.11.13.23298179 Preprint at https://doi.org/10.1101/2023.11.13.23298179 (2023).

10. Sundaram, L. *et al.* Predicting the clinical impact of human mutation with deep neural networks. *Nat Genet* **50**, 1161–1170 (2018).
11. Aaltonen, L. A. *et al.* Pan-cancer analysis of whole genomes. *Nature* **578**, 82–93 (2020).
12. Walsh, M. F. *et al.* Integrating Somatic Variant Data and Biomarkers for Germline Variant Classification in Cancer Predisposition Genes. *Hum Mutat* **39**, 1542–1552 (2018).
13. Castel, P., Rauen, K. A. & McCormick, F. The duality of human oncoproteins: drivers of cancer and congenital disorders. *Nat Rev Cancer* **20**, 383–397 (2020).
14. Nussinov, R., Tsai, C.-J. & Jang, H. How can same-gene mutations promote both cancer and developmental disorders? *Science Advances* **8**, eabm2059 (2022).
15. Dunnett-Kane, V. *et al.* Germline and sporadic cancers driven by the RAS pathway: parallels and contrasts. *Ann Oncol* **31**, 873–883 (2020).
16. Kodaz, H. *et al.* Frequency of Ras Mutations (Kras, Nras, Hras) in Human Solid Cancer. *EURASIAN JOURNAL OF MEDICINE AND ONCOLOGY* **1**, 1–7 (2017).
17. Bennett, J. T. *et al.* Mosaic Activating Mutations in FGFR1 Cause Encephalocraniocutaneous Lipomatosis. *The American Journal of Human Genetics* **98**, 579–587 (2016).
18. Bryant, L. *et al.* Histone H3.3 beyond cancer: Germline mutations in Histone 3 Family 3A and 3B cause a previously unidentified neurodegenerative disorder in 46 patients. *Science Advances* (2020) doi:10.1126/sciadv.abc9207.
19. Popp, B. *et al.* The constitutional gain-of-function variant p.Glu1099Lys in NSD2 is associated with a novel syndrome. *Clin Genet* **103**, 226–230 (2023).

20. Okur, V. *et al.* De novo variants in H3-3A and H3-3B are associated with neurodevelopmental delay, dysmorphic features, and structural brain abnormalities. *npj Genom. Med.* **6**, 1–10 (2021).
21. Valencia, A. M. *et al.* Landscape of mSWI/SNF chromatin remodeling complex perturbations in neurodevelopmental disorders. *Nat Genet* **55**, 1400–1412 (2023).
22. Chang, M. T. *et al.* Accelerating Discovery of Functional Mutant Alleles in Cancer. *Cancer Discov* **8**, 174–183 (2018).
23. Chang, M. T. *et al.* Identifying recurrent mutations in cancer reveals widespread lineage diversity and mutational specificity. *Nat Biotechnol* **34**, 155–163 (2016).
24. Landrum, M. J. *et al.* ClinVar: improving access to variant interpretations and supporting evidence. *Nucleic Acids Res* **46**, D1062–D1067 (2018).
25. Sondka, Z. *et al.* The COSMIC Cancer Gene Census: describing genetic dysfunction across all human cancers. *Nat Rev Cancer* **18**, 696–705 (2018).
26. Hamosh, A., Scott, A. F., Amberger, J. S., Bocchini, C. A. & McKusick, V. A. Online Mendelian Inheritance in Man (OMIM), a knowledgebase of human genes and genetic disorders. *Nucleic Acids Res* **33**, D514-517 (2005).
27. Tavtigian, S. V. *et al.* Modeling the ACMG/AMP variant classification guidelines as a Bayesian classification framework. *Genet Med* **20**, 1054–1060 (2018).
28. Pejaver, V. *et al.* Evidence-based calibration of computational tools for missense variant pathogenicity classification and ClinGen recommendations for clinical use of PP3/BP4 criteria. 2022.03.17.484479 Preprint at https://doi.org/10.1101/2022.03.17.484479 (2022).

29. Pejaver, V. *et al.* Calibration of computational tools for missense variant pathogenicity classification and ClinGen recommendations for PP3/BP4 criteria. *Am J Hum Genet* **109**, 2163–2177 (2022).
30. Cheng, J. *et al.* Accurate proteome-wide missense variant effect prediction with AlphaMissense. *Science* **381**, eadg7492 (2023).
31. McFadden, D. Conditional logit analysis of qualitative choice behavior. *Frontiers in econometrics* (1974).
32. Costain, G. & Andrade, D. M. Third-generation computational approaches for genetic variant interpretation. *Brain* **146**, 411–412 (2023).
33. Schmidt, A. *et al.* Predicting the pathogenicity of missense variants using features derived from AlphaFold2. 2022.03.05.483091 Preprint at https://doi.org/10.1101/2022.03.05.483091 (2022).
34. Horak, P. *et al.* Standards for the classification of pathogenicity of somatic variants in cancer (oncogenicity): Joint recommendations of Clinical Genome Resource (ClinGen), Cancer Genomics Consortium (CGC), and Variant Interpretation for Cancer Consortium (VICC). *Genet Med* S1098-3600(22)00001–6 (2022) doi:10.1016/j.gim.2022.01.001.
35. Rehm, H. L. *et al.* ClinGen — The Clinical Genome Resource. *N Engl J Med* **372**, 2235–2242 (2015).
36. Miranda Durkie *et al.* ACGS Best Practice Guidelines for Variant Classification in Rare Disease 2023. *ACGS* (2023).
37. Hopkins, J. J., Wakeling, M. N., Johnson, M. B., Flanagan, S. E. & Laver, T. W. REVEL Is Better at Predicting Pathogenicity of Loss-of-Function than Gain-of-Function Variants. *Human Mutation* **2023**, e8857940 (2023).

38. Ioannidis, N. M. *et al.* REVEL: An Ensemble Method for Predicting the Pathogenicity of Rare Missense Variants. *Am J Hum Genet* **99**, 877–885 (2016).

39. Pollard, K. S., Hubisz, M. J., Rosenbloom, K. R. & Siepel, A. Detection of nonneutral substitution rates on mammalian phylogenies. *Genome Res* **20**, 110–121 (2010).

40. Siepel, A. *et al.* Evolutionarily conserved elements in vertebrate, insect, worm, and yeast genomes. *Genome Res* **15**, 1034–1050 (2005).

41. Trost, B. *et al.* Genome-wide detection of tandem DNA repeats that are expanded in autism. *Nature* **586**, 80–86 (2020).

42. Turro, E. *et al.* Whole-genome sequencing of patients with rare diseases in a national health system. *Nature* **583**, 96–102 (2020).

43. Boycott, K. M. *et al.* Care4Rare Canada: Outcomes from a decade of network science for rare disease gene discovery. *Am J Hum Genet* **109**, 1947–1959 (2022).

44. Kaplanis, J. *et al.* Evidence for 28 genetic disorders discovered by combining healthcare and research data. *Nature* **586**, 757–762 (2020).

45. Driver, H. G. *et al.* Genomics4RD: An integrated platform to share Canadian deep-phenotype and multiomic data for international rare disease gene discovery. *Hum Mutat* **43**, 800–811 (2022).

46. Tate, J. G. *et al.* COSMIC: the Catalogue Of Somatic Mutations In Cancer. *Nucleic Acids Research* **47**, D941–D947 (2019).

47. Fokkema, I. F. A. C. *et al.* LOVD v.2.0: the next generation in gene variant databases. *Human Mutation* **32**, 557–563 (2011).

48. Genomics England. The National Genomics Research and Healthcare Knowledgebase v5. (2019) doi:doi:10.6084/m9.figshare.4530893.v5.

49. Villani, A. *et al.* The clinical utility of integrative genomics in childhood cancer extends beyond targetable mutations. *Nat Cancer* 1–19 (2022) doi:10.1038/s43018-022-00474-y.

50. Sim, N.-L. *et al.* SIFT web server: predicting effects of amino acid substitutions on proteins. *Nucleic Acids Res* **40**, W452–W457 (2012).

51. Adzhubei, I. A. *et al.* A method and server for predicting damaging missense mutations. *Nat Methods* **7**, 248–249 (2010).

52. Kircher, M. *et al.* A general framework for estimating the relative pathogenicity of human genetic variants. *Nat Genet* **46**, 310–315 (2014).

53. Wu, Y. *et al.* Improved pathogenicity prediction for rare human missense variants. *The American Journal of Human Genetics* **108**, 1891–1906 (2021).

DISPLAY ITEMS

Figure 1. Germline variant and somatic cancer mutation overlap. (A) The presence of either gain-of-function or loss-of-function mutations in cancer driver genes can lead to cancer (left) or rare Mendelian disorders (right) in different contexts. Most cancers result from somatic mutations that accumulate in a tissue-specific manner, whereas germline mutations are present in all cells of the body and cause a type of rare Mendelian disorder (e.g., neurodevelopmental disorder). (B) The *HRAS*^{Q61K} mutation is an example of a known cancer mutation that drives different types of cancers that also causes Costello syndrome, a developmental disorder, when observed as a germline variant. (C) Workflow for extracting cancer mutations from Cancer Hotspots. Recurrent cancer mutations were filtered to 2,447 missense mutations. See main text for details. REVEL scores thresholds correspond to supporting evidence for pathogenicity (PP3) and for benign-ness (BP4). Created with Lucidchart.

Figure 2. Training dataset for supervised learning models. The training dataset is comprised of 13,881 germline missense variants from ClinVar (green), including 691 overlapping with cancer mutations (blue). Different single nucleotide changes causing the same amino acid change were grouped together accounting for the difference in the overlap shown in Figure 1. Variants of uncertain significance (VUS) with REVEL scores ≤ 0.290 were included in the dataset and treated as likely benign/benign (LB/B) variants (see text for justification). LP/P, Likely pathogenic/Pathogenic. Created with BioRender.

Figure 3. Fit of training dataset using supervised learning models. (A) Plot of predicted probabilities of pathogenicity for all likely benign/benign/variant of uncertain significance (LB/B/VUS) and likely pathogenic/pathogenic (LP/P) in the training dataset assigned by the logistic regression model. Mann-Whitney U test: U = 1655893, $n_{LB/B/VUS}$ = 11,644, $n_{LP/P}$ = 2,095. (B) Comparison of predicted probabilities for germline variants with absence or presence of overlap with cancer mutations. Mann-Whitney U test: U = 32029, n_{Absent} = 13,316, $n_{Present}$ = 423. (C) Plot of probability scores of pathogenicity for LB/B/VUS and LP/P in the training dataset assigned by the random forest model. Mann-Whitney U test: U = 6109589, $n_{LB/B/VUS}$ = 11,644, $n_{LP/P}$ = 2,095. (D) Comparison of probability scores for germline variants with absence or presence of overlap with cancer mutations. Mann-Whitney U test: U =12913, n_{Absent} = 13,316, $n_{Present}$ = 423. Created with GraphPad Prism.

Figure 4. Evaluation of supervised learning models. Precision-recall curve comparing the performance of the logistic regression model (blue) and the random forest model (purple) using the (A) test dataset and (B) cross-validation set. The models' performance was evaluated using k-fold cross-validation, with k=8 for logistic regression and k=10 for random forest. AUC, area under the curve.

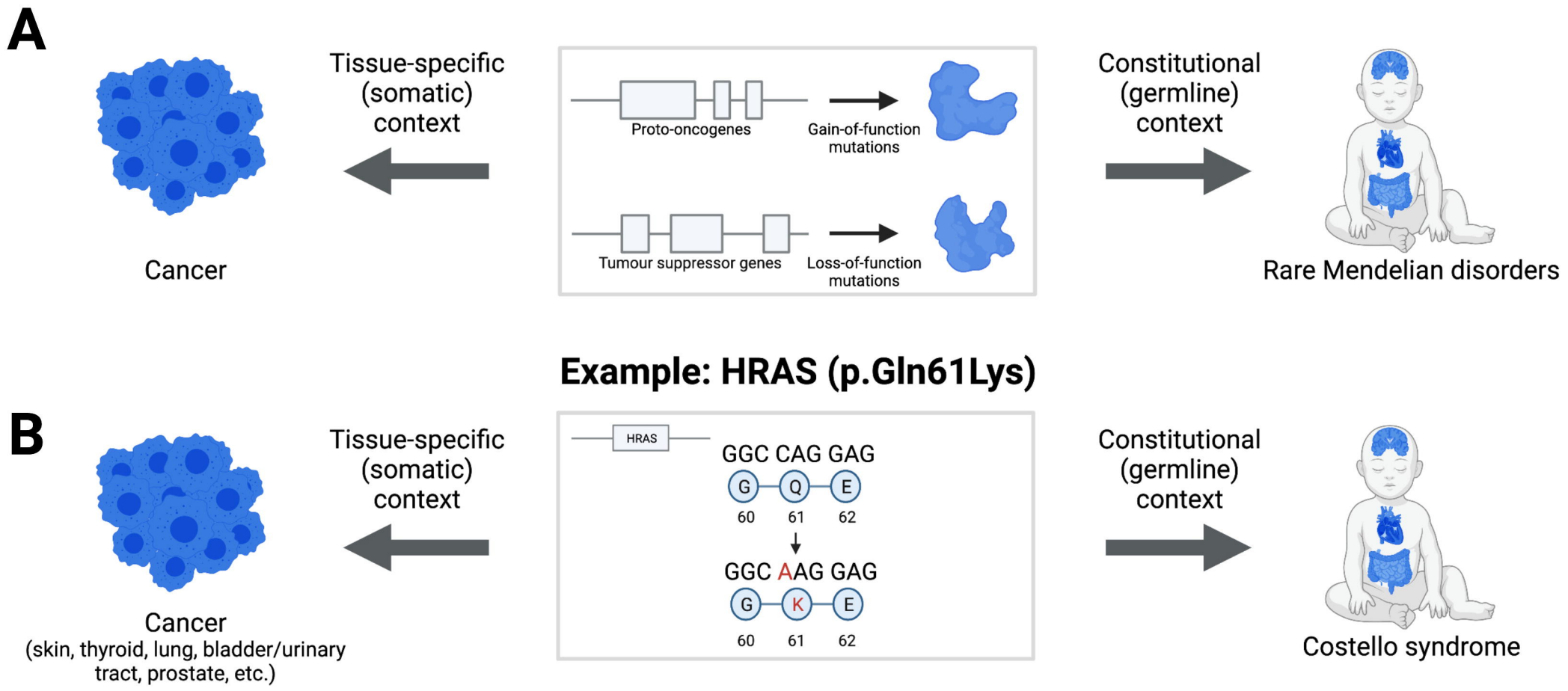
A
Cancer
Tissue-specific (somatic) context
Proto-oncogenes
Gain-of-function mutations
Tumour suppressor genes
Loss-of-function mutations
Constitutional (germline) context
Rare Mendelian disorders
Example: HRAS (p.Gln61Lys)
B
Cancer
(skin, thyroid, lung, bladder/urinary tract, prostate, etc.)
Tissue-specific (somatic) context
HRAS
GGC CAG GAG
G Q E
60 61 62
GGC AAG GAG
G K E
60 61 62
Constitutional (germline) context
Costello syndrome

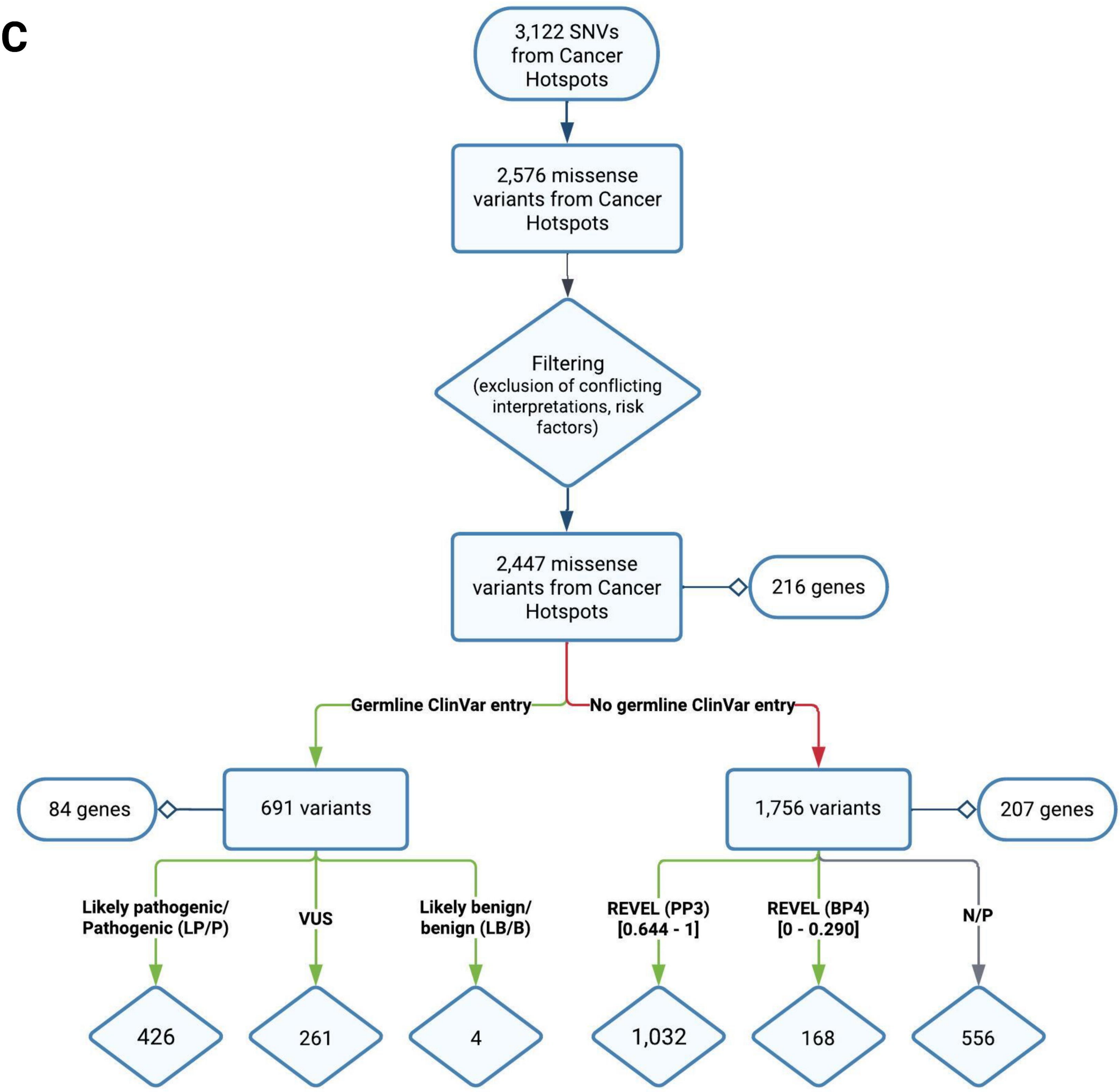
C
3,122 SNVs from Cancer Hotspots
2,576 missense variants from Cancer Hotspots
Filtering
(exclusion of conflicting interpretations, risk factors)
2,447 missense variants from Cancer Hotspots
216 genes
Germline ClinVar entry
No germline ClinVar entry
84 genes
691 variants
1,756 variants
207 genes
Likely pathogenic/ Pathogenic (LP/P)
VUS
Likely benign/ benign (LB/B)
REVEL (PP3) [0.644 - 1]
REVEL (BP4) [0 - 0.290]
N/P
426
261
4
1,032
168
556

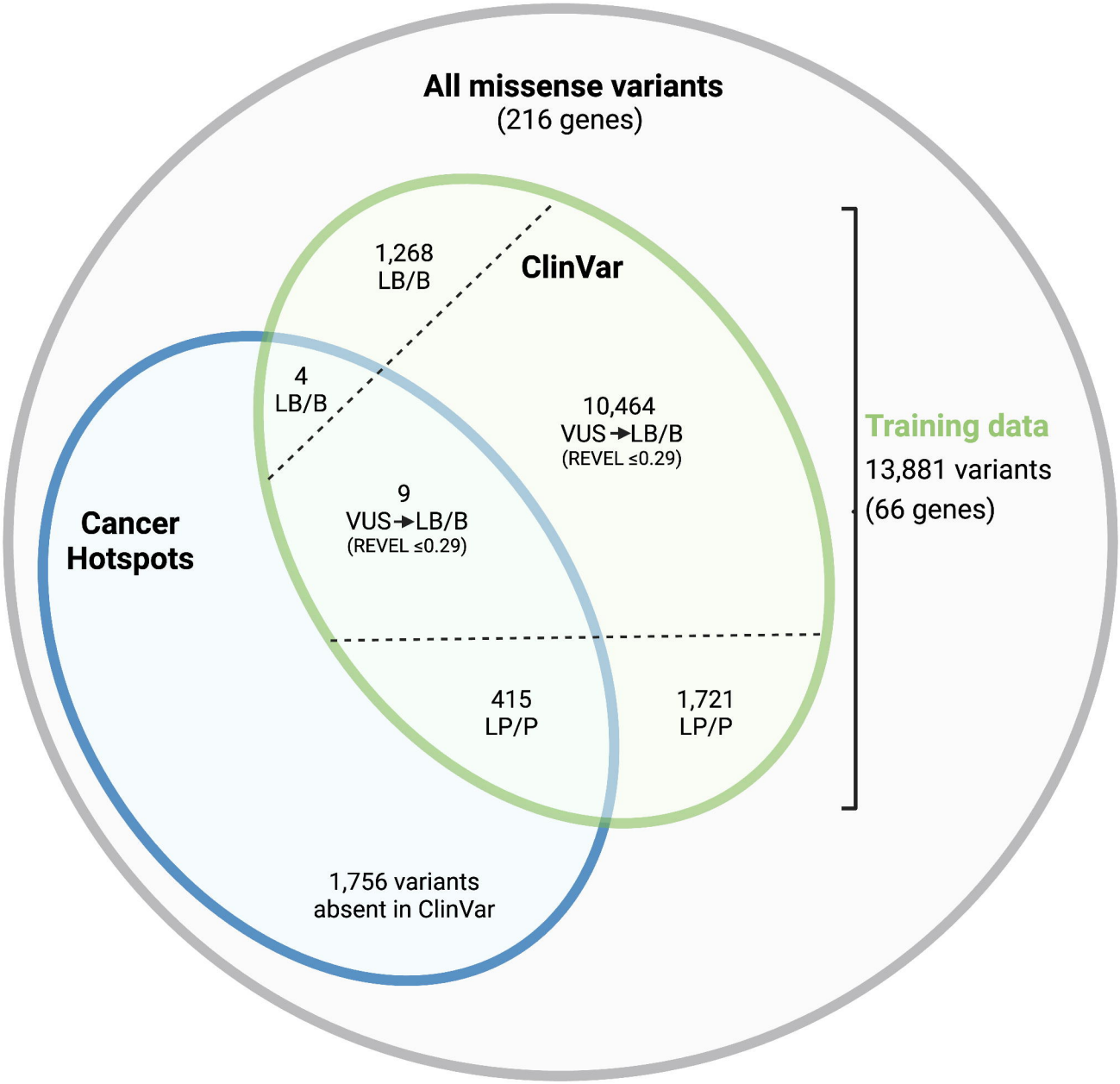
All missense variants
(216 genes)
ClinVar
1,268
LB/B
4
LB/B
10,464
VUS→LB/B
(REVEL ≤0.29)
9
VUS→LB/B
(REVEL ≤0.29)
Cancer
Hotspots
415
LP/P
1,721
LP/P
1,756 variants
absent in ClinVar
Training data
13,881 variants
(66 genes)

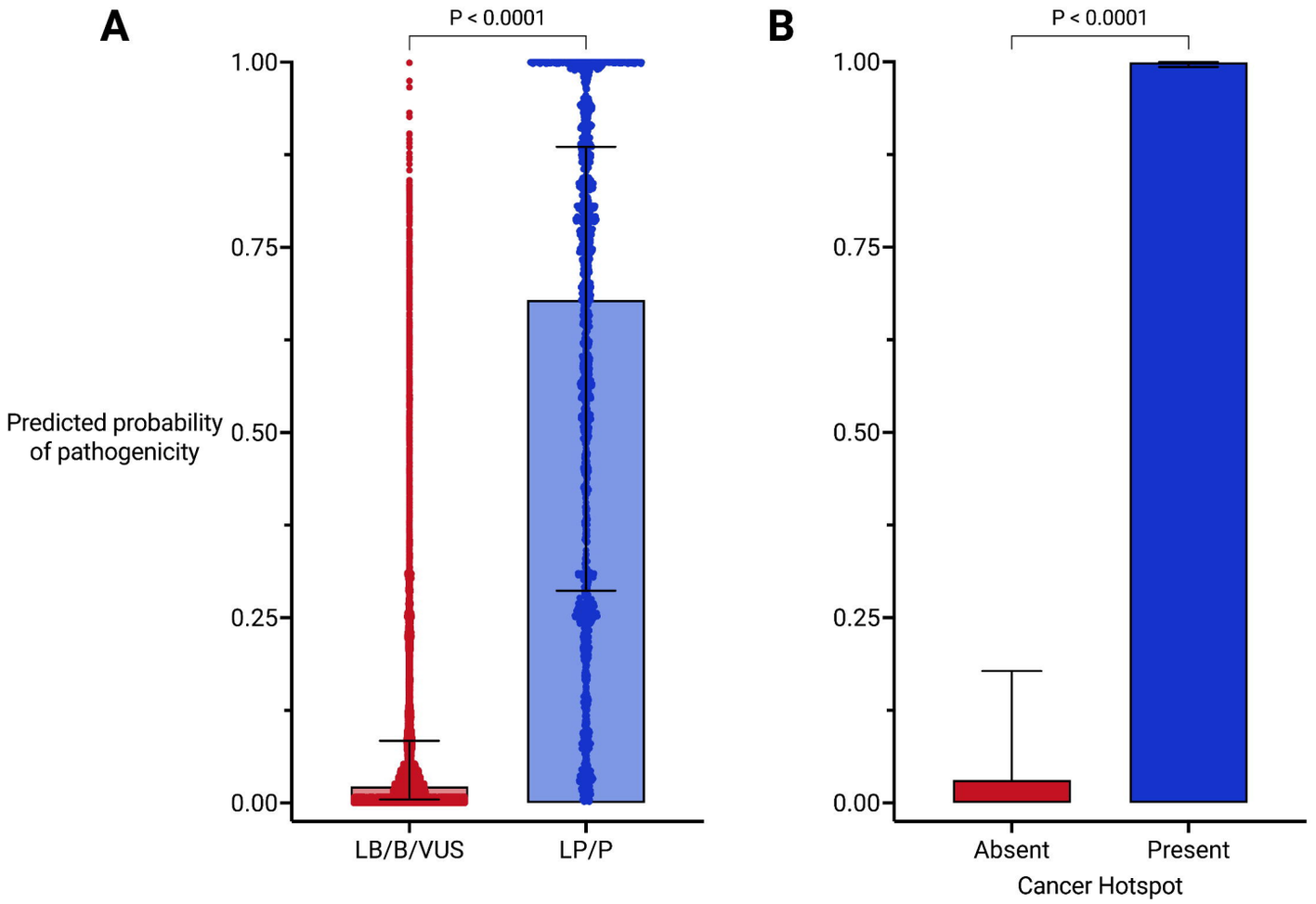

Logistic Regression Model

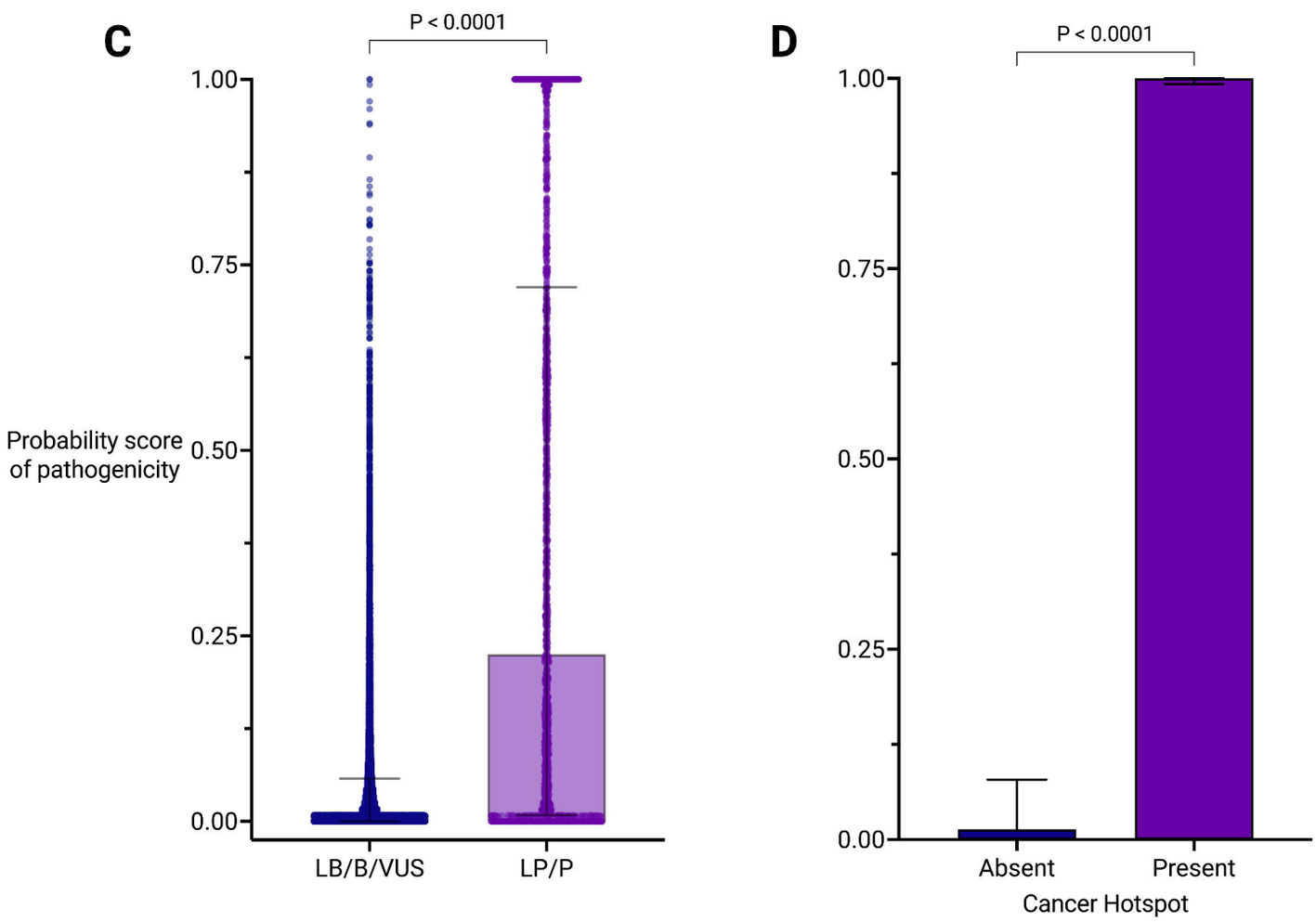

Random Forest Model

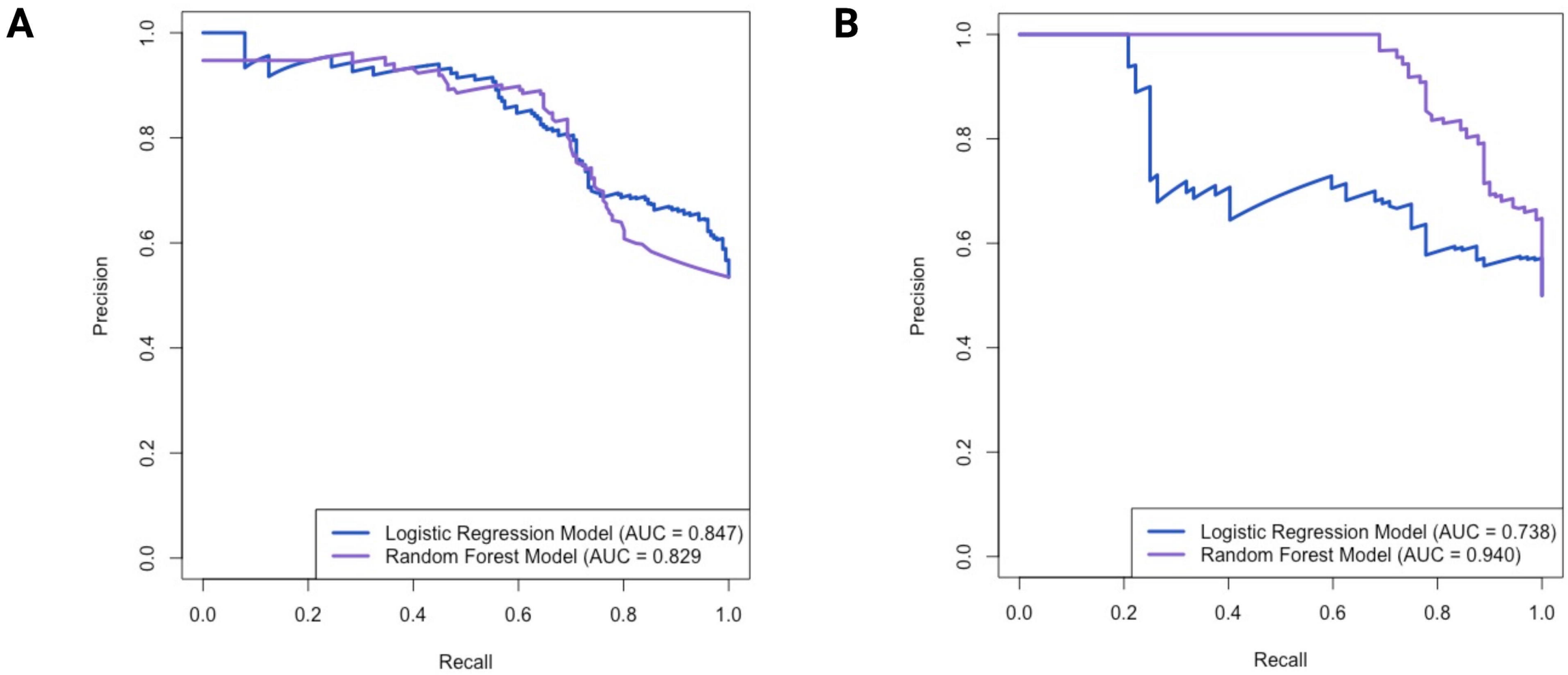
A
Precision
Recall
0.0
0.2
0.4
0.6
0.8
1.0
Logistic Regression Model (AUC = 0.847)
Random Forest Model (AUC = 0.829
B
Precision
Recall
Logistic Regression Model (AUC = 0.738)
Random Forest Model (AUC = 0.940)